Numerical Simulation of a Rotary Desiccant Wheel

G. Diglio*, P. Bareschino, G. Angrisani, M. Sasso and F. Pepe
Dipartimento di Ingegneria, Università degli Studi del Sannio, Piazza Roma 21, 82100 Benevento, Italy
*Corresponding author: Piazza Roma 21, 82100 Benevento, Italy, diglio@cheapnet.it

Abstract: A general predictive model and an analysis of performances under various design and operational conditions for a desiccant wheel was developed with the aid of COMSOL Multhipysics. A one dimensional coupled heat and mass transfer model, combined with the classical Linear Driving Force (LFD) approximation, was implemented taking into account the dependence of the thermodynamic and transport properties of humid air with temperature. Temperature and humidity profiles at the exit of the wheel during the dehumidification process were obtained and analyzed for various process and regeneration time, temperature and moisture content of regeneration air and process air flow rate.

Keywords: Desiccant Wheel, Adsorption, Heat and Mass transfer.

1. Introduction

Desiccant cooling systems (DCSs) have been used in the U.S.A. since the early '30s, mainly for industrial applications in which significant economic benefits could be achieved from an accurate humidity control.

The core unit of a DCS is the dehumidifying device, in most cases a wheel made of inert material coated with an adsorbent (silica gel in the present work). Two sections of the wheel can be identified: a process section, through which air to be dehumidified is passed, and a regeneration section, where water vapor is removed from the adsorbent by means of a dry and hot air counter-flow, as shown in Fig. 1.

More recently, as a consequence of the development of materials with higher adsorption capacity and smaller energy request for regeneration, applications of DCSs for environmental conditioning increased. Growing attention to environmental safety also contributes to diffusion of these systems, since water is used as refrigerant instead of those used in conventional systems, such as HCFC and HFC.

Since adsorption is an exothermic process, dehumidified air has to be cooled before it can be supplied into a part of a building: energy saving and environmental impact reduction that DCSs can achieve are high when the desiccant material can be effectively regenerated by a low-temperature thermal energy carrier. Air conditioning through the use of DCSs could be seen as an alternative or as a supplement to traditional systems in order to reduce their energy cost since, in most cases, they are energetically coupled with "free" energy sources, such as solar collectors or "waste" heat from conversion processes.

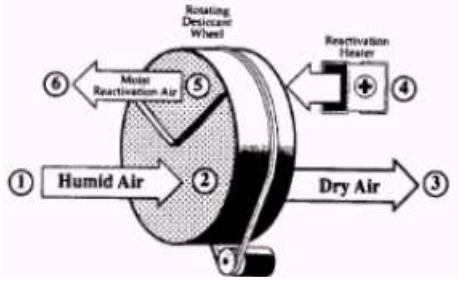

Figure 1. Principle of operation of the Desiccant Wheel

2. Governing Equations

A sketch of the desiccant wheel and of the control volume for the model developed are shown in Fig. 2.

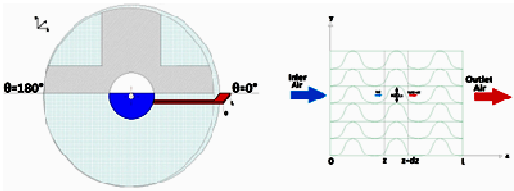

Figure 2. Sketch of desiccant wheel and control volume adopted in the model.

Based on the model developed by Ahmed *et al.* [2] and under the assumptions that:

(1) air flow is one dimensional;
(2) thermal and physical properties of the silica gel do not change in the range of operating temperatures;

(3) whole system is adiabatic;
(4) temperature and moisture content does not change with radial position;
(5) classical Linear Driving Force Approximation (LFD) for the mass balance in the desiccant material can be used;

a model for both the dehumidification (DP) and regeneration phases (RP) was written as follows:

2.1 Mass balances

Two mass balance equations can be written, the first one expressing variations of the gas moisture content (gas-side mass-balance, GSMB) and the second one for moisture content variations in the desiccant material (solid-side mass-balance, SSMB).

SSMB, given the fifth assumption, can always be expressed as:

$$\frac{\partial M}{\partial t} = K(M_e - M) \tag{1}$$

During dehumidification phase, GSMB can be written as:

$$\rho_a \frac{\partial w}{\partial t} + \rho_a V_a \frac{\partial w}{\partial z} = \rho_a D_s \frac{\partial^2 w}{\partial z^2} - \frac{\varepsilon_d \rho_d}{\varepsilon_a} \frac{\partial M}{\partial t} \tag{2}$$

while, during regeneration phase, the same balance has to be expressed as:

$$\rho_a \frac{\partial w}{\partial t} - \rho_a V_r \frac{\partial w}{\partial z} = \rho_a D_s \frac{\partial^2 w}{\partial z^2} - \frac{\varepsilon_d \rho_d}{\varepsilon_a} \frac{\partial M}{\partial t} \tag{3}$$

In DP, Eq.s (1) and (2) were solved with the following I.C.s and B.C.:

$$M(z, t_{proc}) = M_{in} \tag{4}$$

$$w(z, t_{proc}) = w_{amb} \tag{5}$$

$$w(0, t) = w_{amb} \tag{6}$$

$$\left.\frac{\partial w}{\partial t}\right|_{L,t} = 0 \tag{7}$$

During RP, Eq.s (1) and (3) with the following associated I.C.s and B.C.s were considered:

$$M(z, t_{reg}) = M_{out} \tag{8}$$

$$w(z, t_{reg}) = w_{out} \tag{9}$$

$$w(L, t) = w_{reg} \tag{10}$$

$$\left.\frac{\partial w}{\partial t}\right|_{0,t} = 0 \tag{11}$$

2.2 Global Energy balance

Energy conservation during adsorption phase can be expressed as

$$\left((1-\varepsilon_d)\rho_a c_{pa} + \frac{\varepsilon_d}{A}\rho_d c_{pd}\right)\frac{\partial T_a}{\partial t} + (1-\varepsilon_d)\rho_a c_{pa} V_a \frac{\partial T_a}{\partial z} = (1-\varepsilon_d)k_a \frac{\partial^2 T_a}{\partial z^2} + \frac{h_s}{A}\varepsilon_d \rho_d \frac{\partial M}{\partial t} \tag{12}$$

while, during regeneration phase, the same balance has to be:

$$\left((1-\varepsilon_d)\rho_a c_{pa} + \frac{\varepsilon_d}{A}\rho_d c_{pd}\right)\frac{\partial T_a}{\partial t} - (1-\varepsilon_d)\rho_a c_{pa} V_a \frac{\partial T_a}{\partial z} = (1-\varepsilon_d)k_a \frac{\partial^2 T_a}{\partial z^2} + \frac{h_s}{A}\varepsilon_d \rho_d \frac{\partial M}{\partial t} \tag{13}$$

For Eq. 12, initial and boundary conditions were:

$$T_a(z, t_{proc}) = T_{amb} \tag{14}$$

$$T_a(0, t) = T_{amb} \tag{15}$$

$$\left.\frac{\partial T_a}{\partial t}\right|_{L,t} = 0 \tag{16}$$

for Eq. 13, I.C. and B.C.s were:

$$T_a(z, t_{reg}) = T_{out} \tag{17}$$

$$T_a(L, t) = T_{reg} \tag{18}$$

$$\left.\frac{\partial T_a}{\partial t}\right|_{0,t} = 0 \tag{19}$$

2.3 Additional Equations

In order to have a well posed PDEs system, some auxiliary equation have to be provided.

Kodama *et al*. [3] correlation was adopted in order to express adsorption equilibrium on silica gel:

$$M_e = 0.24\theta^{1/1.5} \tag{20}$$

Adsorption heat was calculated according to [1] as:

$$h_s = 3500 - 12400w \rightarrow w \le 0.05 \tag{21}$$

$$h_s = 2950 - 1400w \rightarrow w > 0.05 \tag{22}$$

According to [3], surface diffusivity can be written as:

$$D_s = 2.27\times10^{-7}\, exp(-h_s / RT) \tag{23}$$

Effective mass transfer coefficient was expressed according to [4] as:

$$K = \frac{15 D_s}{r^2} \tag{24}$$

Water saturation pressure as a function of temperature was calculated by means of Antoine's equation.

3. Use of COMSOL Multiphysics

The model above was implemented in COMSOL Multiphysics. "Transport of Concentrated Species" interface to solve gas-phase mass-transfer and "Heat Transfer in Porous Media" interface to solve overall energy balance were used. "Classical PDEs - Convection-Diffusion Equation" interface to solve solid-phase mass-transfer was employed.

Moreover, properties of moist air as a function of temperature from COMSOL model library have been used.

3.1 Parameters, variables and functions

First of all, model parameters have been defined. All defined parameters and their values are given in Appendix.

Eq.s (20)-(24) and Antoine's equation were defined as variables.

3.2 Geometry and Mesh

Given the first assumption, chosen geometry was one-dimensional. The endpoint at 0 was the inlet during the dehumidification phase while the endpoint at *L* was the outlet, *vice-versa* for the regeneration phase as shown in Fig. 3.

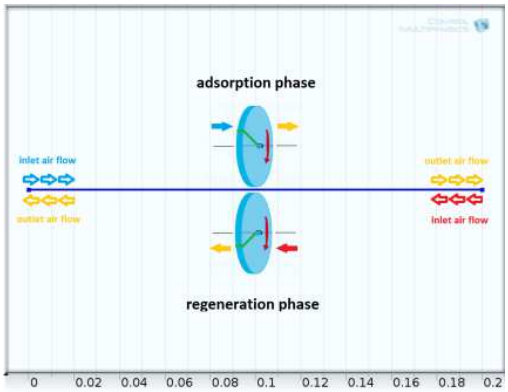

Figure 3. Geometry during adsorption and regeneration phase.

Mesh has been set as "physics-controlled mesh" for Sequence Type and "Extremely Fine" for Element Size. Consequently, a mesh with 100 elements was obtained. As a consequence, the system gets 403 degrees of freedom.

3.3 Transport of Concentrated Species

To solve gas-phase mass-transfer, i.e. Eq. (2) for adsorption phase and Eq. (3) for regeneration phase, this physic was used.

Main interface inputs are shown in Table 1.

"Inflow" and "Outflow" nodes were used in order to express boundary conditions.

Table 1: Data Inputs for "Transport in Concentrated Species"

Interface input	Value
u	V_a
T	*from Heat Transfer in Porous Media*
ρ	*from Heat Transfer in Porous Media*
M_w	*0.018016 [kg/mol]*
M_a	*0.028964 [kg/mol]*
D_{ik}	D_s

3.4 Heat Transfer in Porous Media

Equation (12) during DP and equation (13) during RP were solved using this physic.

"Temperature" and "Outflow" nodes were used to express associated boundary conditions.

Interface inputs are shown in the following Table 2.

Table 2: Data Inputs for "Heat Transfer in Porous Media"

Interface input	Value
u	$(1-\varepsilon_d)V_a$
P	P
Fluid type	*Moist Air*
Vapor Mass Fraction	w
θ_p	ε_d
k_p	*0*
ρ_p	ρ_d/A
$C_{p,p}$	c_{pd}

3.5 Classical PDEs: Convection-Diffusion Equation

To solve Eq. (1), this physic was used. "Mass Fraction" was chosen as dependent variable and "Specific Dissipation Rate" was chosen as source term. Interface inputs are shown in Table 3.

Table 3: Data Inputs for "Convection-Diffusion Equation"

Interface input	Value
c	*0*
β	*0*
f	$K(M_e-M)$
d_a	*1*

3.6 Initial values and Boundary Conditions

"Base-case" values of design and operational parameters were reported in Appendix. Computations are carried on for a sufficiently large number of cycles in order to approach a cyclic steady state profile in both adsorption and regeneration process. Dehumidification phase was chosen as "starting-point".

When DP ended, simulation was stopped and last time values of all variables were taken as initial values for regeneration phase. This procedure has been iterated for each cycle.

4. Results

4.1 Comparison with literature model

Figs. 4 and 5 show a comparison between moisture content and temperature of air leaving the system during dehumidification and regeneration phases calculated according to the model developed herein and to one derived from literature [5].

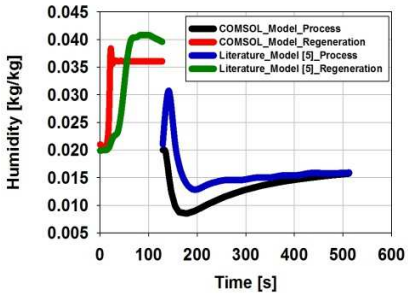

Figure 4. Moisture removed during adsorption and regeneration process.

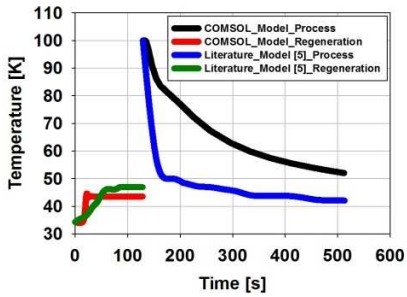

Figure 5. Outlet air temperature during adsorption and regeneration process.

Overall trend was the same; deviations between calculated data are mainly due to the fact that literature model [5] does not take into account any variation of moist air properties with temperature. Furthermore, literature model was referred to a single channel of the wheel.

4.2 Parametric study

Figs. 6 and 7 report temperature and humidity time profiles at the exit of the wheel for the "base-case".

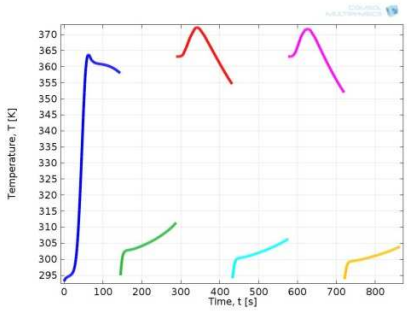

Figure 6. Air temperature time profiles at the exit of the wheel, "base-case".

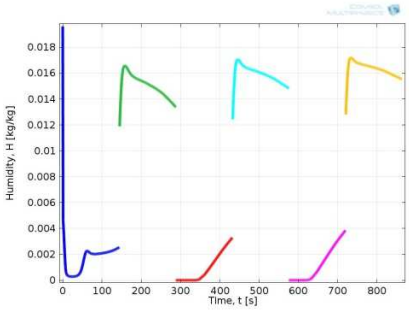

Figure 7. Air humidity time profiles at the exit of the wheel, "base-case".

Starting from base-case values and changing one parameter at a time, influence of process parameters on of temperature (T) and humidity content (H) of air at the exit of the wheel was evaluated.

Figs. 8 and 9 show mean values of T and H as a function of the process/regeneration time ratio.

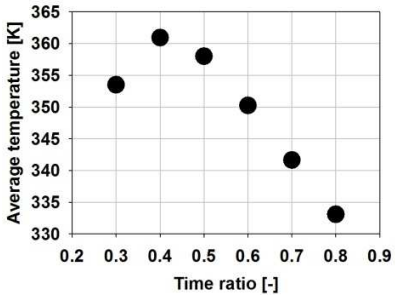

Figure 8. Time averaged process air temperature at the exit of the wheel as a function of process/regeneration time ratio.

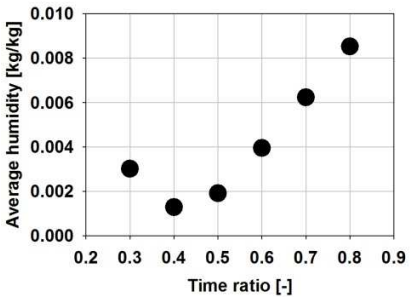

Figure 9. Time averaged process air humidity at the exit of the wheel as a function of process/regeneration time ratio.

An optimum time ratio can clearly be identified: if time ratio is equal to 0.4, a minimum in H can be reached. For time ratio lower than 0.4, too short and less effective dehumidification phases took place; on the oher hand, longer time ratios lead to too short and less effective regeneration period.

Figs. 10 and 11 show mean value of T and H as a function of regeneration air temperature.

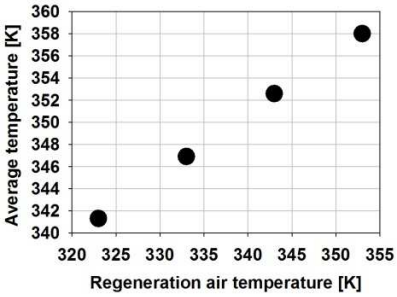

Figure 10. Time averaged process air temperature at the exit of the wheel as a function of regeneration air temperature.

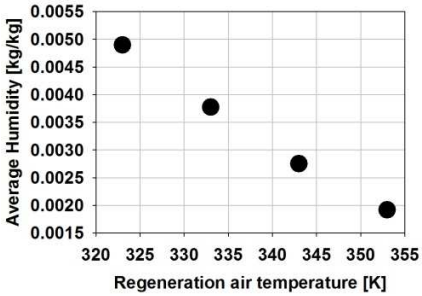

Figure 11. Time averaged process air humidity at the exit of the wheel as a function of regeneration air temperature.

As the regeneration temperature increases the amount of water vapor removed from the air stream increases. In fact, low regeneration air temperature leads to higher relative humidity and consequently to higher capacity of desiccant material of keeping water. The result is a poor dehumidification capacity due to the reduced mass transfer between the wet air and the adsorbent layer.

Figs. 12 and 13 show mean value of T and H as a function of regeneration air humidity.

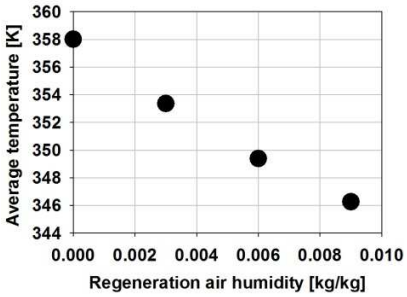

Figure 12. Time averaged process air temperature at the exit of the wheel as a function of regeneration air humidity.

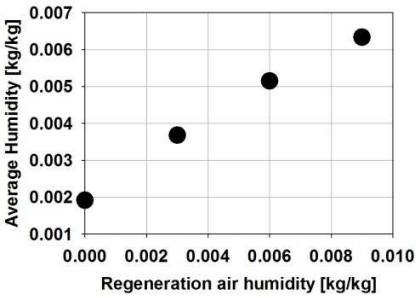

Figure 13. Time averaged process air humidity at the exit of the wheel as a function of regeneration air humidity.

In this case, as the regeneration air humidity increases, dehumidification capacity of the wheel decreases. In fact, the lower is the inlet regeneration air humidity, the higher is the dehumidification capacity. This effect is due to higher mass transfer driving force during the regeneration period which leads to higher moisture removal from the desiccant matrix.

Figs. 14 and 15 show mean value of *T* and *H* as a function of process air flow.

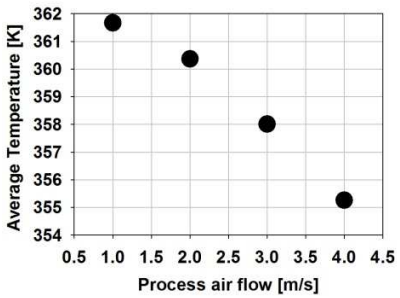

Figure 14. Time averaged process air temperature at the exit of the wheel as a function of process air flow.

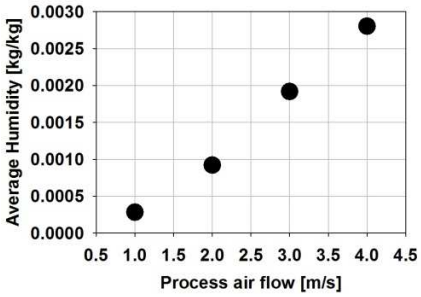

Figure 15. Time averaged process air humidity at the exit of the wheel as a function of process air flow.

Clearly, as the process air flow increases the dehumidification capacity of the wheel decreases as a consequence of smaller gas residence times.

6. Conclusions

A one dimensional coupled heat and mass transfer model, based on the model developed by Ahmed *et al.* [2], combined with the classical Linear Driving Force approximation and taking into account dependence of thermodynamic properties of moist air from temperature, was implemented in COMSOL Multiphysics.

A comparison with a literature model has been carried out and a good agreement were achieved.

Different simulations have been carried out in order to investigate the effect of the variation of operational parameters on moisture content and temperature of air leaving the system. Numerical results show that there is an optimum value of process-to-regeneration time ratio beyond which adsorption/regeneration process becomes ineffective.

Fine tuning of the model with data obtained from an experimental facility located in the "Università degli Studi del Sannio" laboratory and operated under different conditions is ongoing.

7. References

1. TS Ge, Y Li, RZ Wang, YJ Dai, A review of the mathematical models for predicting rotary desiccant wheel, *Renewable and Sustainable Energy Reviews*, **12**, 1485-1528 (2008)
2. MH Ahmed, NM Kattab, M Fouad, Evaluation and optimization of solar desiccant wheel performance, *Renewable Energy*, **30**, 305-325 (2005)
3. A Kodama, T Hirayama, M Goto, T Hirose, RE Critoph, The use of psychrometric charts for the optimization of a thermal swing desiccant wheel, *Applied Thermal* Engineering, **21**, 1657-1674 (2001)
4. A Sakoda, M Suzuki, Simultaneous transport of heat and mass in closed type adsorption cooling system utilizing solar heat, *Journal of Solar Energy Engineering*, **108**, 239-251 (ASME 1986)
5. XJ Zhang, YJ Dai, RZ Wang, A simulation study of heat and mass transfer in a honeycombed rotary desiccant dehumidifier, *Applied Thermal Engineering*, **23**, 989-1003 (2003)
6. G Angrisani, C Roselli, M Sasso, Effect of rotational speed on the performances of a desiccant wheel, *Applied Energy*, **104**, 268-275 (2013)

9. Appendix

Nomenclature

L: thickness of the wheel, m
P: atmospheric pressure, Pa

ε: air void fraction, -
ε_d: silica gel fraction volume, -
A: multiplicative constant, -
Φ: air relative humidity, -
P_{sat}: saturation pressure, Pa
w: air humidity ratio, $g_{water}/kg_{moist\ air}$
M: moisture content of silica gel, $kg_{water}/kg_{silica\ gel}$
M_e: equilibrium moisture content of silica gel, $kg_{water}/kg_{silica\ gel}$
T_a: air temperature, K
V_a: process air velocity, m/s
V_r: regeneration air velocity, m/s
h_s: heat of adsorption, kJ/kg
D_s: surface diffusion coefficient, m^2/s
K: effective mass transfer coefficient, 1/s
R: gas constant, J/kgK
ρ_d: silica gel density, kg/m^3
c_{pd}: specific heat of silica gel, J/kgK
c_{pa}: specific heat of moist air, J/kgK
k_a: thermal conductivity of moist air, W/mK
ρ_a: moist air density, kg/m^3
M_{in}: initial moisture content of silica gel, $kg_{water}/kg_{silica\ gel}$
T_{amb}: ambient temperature, K
T_{req}: regeneration temperature, K
w_{amb}: ambient humidity ratio, $g_{water}/kg_{moist\ air}$
w_{req}: regeneration humidity ratio, $g_{water}/kg_{moist\ air}$
r: average radius of the silica gel grain, m
t_{proc}: process time, s
t_{req}: regeneration time, s

COMSOL Model Parameters

L = 0.2 m
P = 1 atm
ε = 0.6
ε_d = 0.7
$A = \varepsilon/(1-\varepsilon_d)$
ρ_d = 720 kg/m^3
c_{pd} = 921 J/kgK
$r = 10^{-10}$ m
M_{in} = 5.17 $g_{water}/kg_{silica\ gel}$

COMSOL Model Input – "Base Case"

t_{proc} = 144 s
t_{req} = 144 s
w_{amb} = 20 g/kg
w_{req} = 0 g/kg
T_{amb} = 293 K
T_{req} = 353 K
V_a = 3 m/s
V_r = *3 m/s*